Notes

Contribution from the Section de Chimie,
Université de Lausanne, CH-1005 Lausanne, Switzerland,
Laboratoire de Chimie de Coordination,
associé au CNRS (UA 416),
Université Louis Pasteur, F-67070 Strasbourg Cedex, France,
and Istituto di Strutturistica Chimica,
Centro di Studio per la Strutturistica Diffrattometrica del CNR,
Università di Parma, I-43100 Parma, Italy

Diastereoselective Synthesis of the Bis(phosphino enolato)nickel(II) Complex $cis\text{-}\{\overline{\mathrm{Ni[Ph_2PCH{=}C(O}}\mathrm{)Fe(\eta\text{-}C_5H_5)(CO)(PPh_3)]_2}\}$, Derived from $(\eta\text{-}C_5H_5)Fe(CO)(PPh_3)C(O)CH_2PPh_2$, and the Corresponding Crystal Structures

Pietro Berno,[†] Pierre Braunstein,*[,‡] Carlo Floriani,*[,†]
Angiola Chiesi-Villa,[§] and Carlo Guastini[§]

Received June 5, 1990

By virtue of the chiral auxiliary $[Fe(\eta\text{-}C_5H_5)(CO)(PPh_3)]$ = [Fe], the acetyl complex $[Fe]{-}C(O)CH_3$[1] (**1**) has been used in its enolato form $[Fe]{-}C(O)CH_2^-$ for the stereoselective delivery of the acyl fragment.[2] Its reactivity and stereoselectivity are determined mainly by the nature of the countercation M.[2,3] Bonding modes A and B of the enolato anion to a transition-metal ion have been reported.[3] Stimulated by the recent discovery of a potentially general route to functional keto or ester phosphine ligands $R_2PCH_2C(O)Z$ (e.g., Z = Ph, OEt) of stoichiometric and catalyst interest, by coupling of R_2PCl with the corresponding lithium enolate selectively at the carbon center,[5] we have investigated the reactions shown in Scheme I, which lead to the new bimetallic enolates C (X = PPh_2).

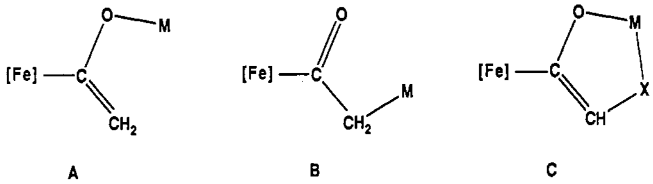

Experimental Section

All operations were carried out under an atmosphere of nitrogen by using standard Schlenk techniques. Solvents were dried and deoxygenated by using standard methods prior to use.

Preparation of $(\eta\text{-}C_5H_5)Fe(CO)(PPh_3)C(O)CH_2PPh_2$ (3). Complex **1** (19.30 g, 42.13 mmol) was dissolved in THF (200 mL). The yellow solution was cooled to −78 °C and LiBu (1.64 M in *n*-hexane, 25.4 mL, 1 equiv) was added. The color changed immediately to dark red, and the solution was stirred for 1 h at −78 °C. A THF (30 mL) solution of $ClPPh_2$ (freshly distilled under reduced pressure, 7.8 mL, 1 equiv) was added dropwise. During the addition, the color changed to orange-yellow. The solution was stirred overnight at room temperature. The solvent was evaporated under reduced pressure, and the residue was extracted with Et_2O (250 mL), affording a yellow microcrystalline product (20.34 g, 76%). Anal. Calcd for $C_{38}H_{32}FeO_2P_2$ (**3**): C, 71.49; H, 5.05; P, 9.70. Found: C, 71.09; H, 5.58; P, 9.66. ^1H NMR (200 MHz, CD_2Cl_2): δ 7.72–7.31 (m, 25 H, Ph), 4.54 (d, 5 H, Cp, $^3J(P{-}H) = 1.22$ Hz), 4.04 (dd, 1 H, PCH^A, $J(H{-}H) = 15.5$ Hz, $^2J(P{-}H) = 1.6$ Hz), 3.44 (dd, 1 H, PCH^B, $J(H{-}H) = 15.5$ Hz, $^2J(P{-}H) = 0.9$ Hz). $^{31}P\{^1H\}$ NMR (CD_2Cl_2): δ 75.2 (s, P1), −20.6 (s, P2). IR (Nujol): ν(CO) 1918 (vs), 1592 (s) cm^{-1}.

Scheme I

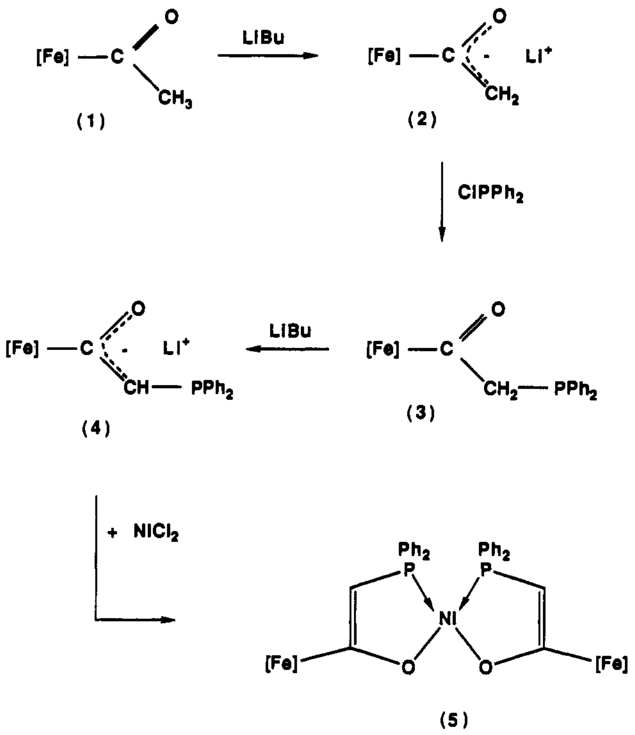

[Fe] ≡ FeCp(CO)(PPh₃)

Preparation of $cis\text{-}\{\overline{\mathrm{Ni[Ph_2PCH{=}C(O}}\mathrm{)Fe(\eta\text{-}C_5H_5)(CO)(PPh_3)]_2}\}$ (5). Complex **3** (4.588 g, 7.18 mmol) was dissolved in THF (100 mL). The solution was cooled to −78 °C, and then LiBu (1.64 M in *n*-hexane, 4.5 mL, 1 equiv) was added. The color changed immediately to cherry red. The solution was stirred for 1 h at −78 °C, and $NiCl_2$ (0.585 g, 4.28 mmol) was added. The mixture was stirred overnight at room temperature, and then the solvent was evaporated. The ^1H NMR spectrum of the crude product showed a 70:30 *RS*,*SR*:*RR*,*SS* diastereomeric ratio. The solid was extracted with Et_2O (150 mL) in order to remove LiCl. The ether solution was reduced to 50 mL, and *n*-hexane was added, affording **5** (4.12 g, 86%). The resulting red-orange crystalline solid

---

[†] Université de Lausanne.

[‡] Université Louis Pasteur.

[§] Università di Parma.

(1) (a) Green, M. L. H.; Hurley, C. R. *J. Organomet. Chem.* **1967**, *10*, 188. (b) Bibler, J. P.; Wojcicki, A. *Inorg. Chem.* **1966**, *5*, 889.

(2) See for example: (a) Blackburn, B. K.; Davies, S. G.; Whittaker, M. In *Stereochemistry of Organometallic and Inorganic Compounds*; Bernal, I., Ed.; Elsevier: Amsterdam, New York, 1989; Vol. III, p 141. (b) Blackburn, B. K.; Davies, S. G.; Sutton, K. H.; Whittaker, M. *Chem. Soc. Rev.* **1988**, *17*, 147. Liebeskind, L. S.; Welker, M. E.; Fengl, R. W. *J. Am. Chem. Soc.* **1986**, *108*, 6328. Davies, S. G. *Pure Appl. Chem.* **1988**, *60*, 13; *Chem. Br.* **1989**, 268.

(3) Burkhardt, E. R.; Doney, J. J.; Slough, G. A.; Stack, J. M.; Heathcock, C. H.; Bergman, R. G. *Pure Appl. Chem.* **1988**, *60*, 1. Additional leading references: Heathcock, C. H. In *Asymmetric Synthesis*; Morrison, J. D., Ed.; Academic Press: New York, 1984; Vol. 3, p 111. Evans, D. A.; Nelson, J. V.; Taber, T. R. In *Topics in Stereochemistry*; Allinger, N. L., Elich, E. L., Wilen, S. H., Eds.; Wiley: New York, 1982; Vol. 13, p 1. Reetz, M. T.; *Organotitanium Reagents in Organic Synthesis*; Springer: Berlin, 1986; Chapter 5.3. Weidmann, B.; Seebach, D. *Angew. Chem., Int. Ed. Engl.* **1983**, *22*, 31. Davies, S. G.; Dordor-Hedgecock, I. M.; Warner, P.; Jones, R. H.; Prout, K. *J. Organomet. Chem.* **1985**, *285*, 213. Brown, S. L.; Davies, S. G.; Warner, P.; Jones, R. H.; Prout, K. *J. Chem. Soc., Chem. Commun.* **1985**, 1446. Slough, G. A.; Bergman, R. G.; Heathcock, C. H. *J. Am. Chem. Soc.* **1989**, *111*, 938.

(4) (a) Weinstock, I.; Floriani, C.; Chiesi-Villa, A.; Guastini, C. *J. Am. Chem. Soc.* **1986**, *108*, 8298. (b) Berno, P.; Floriani, C.; Chiesi-Villa, A.; Guastini, C. *Organometallics* **1990**, *9*, 2185.

(5) Nobel, D. Thèse de Docteur-Ingénieur, Université Louis Pasteur, Strasbourg, France, 1987. Bouaoud, S.-E.; Braunstein, P.; Grandjean, D.; Matt, D.; Nobel, D. *Inorg. Chem.* **1986**, *25*, 3765.

0020-1669/91/1330-1407$02.50/0

Table I. Crystallographic Data for $(\eta\text{-}C_5H_5)Fe(CO)(PPh_3)C(O)CH_2PPh_2$ (**3**) and *cis*-$\{Ni[Ph_2PCH{=}C(O)Fe(\eta\text{-}C_5H_5)(CO)(PPh_3)]_2\}$ (**5**)

formula	$C_{38}H_{32}FeO_2P_2$ (**3**)	$C_{76}H_{62}Fe_2NiO_4P_4\cdot 2CH_2Cl_2$ (**5**)
fw	638.5	1503.5
a, Å	10.300 (1)	17.180 (1)
b, Å	14.266 (1)	17.991 (1)
c, Å	21.914 (2)	12.530 (2)
α, deg	90	107.11 (1)
β, deg	90	100.91 (1)
γ, deg	90	86.74 (1)
V, Å^3	3220.0 (5)	3634.5 (5)
Z	4	2
space group	$P2_12_12_1$	$P\bar{1}$
T, °C	25	25
λ, Å	0.71069	0.71069
ρ(calcd), g/cm^3	1.317	1.374
μ, cm^{-1}	5.96	9.33
R	0.034	0.062
R_w	unit weights	unit weights

showed a diastereomeric ratio almost unchanged. Then the solid was recrystallized from THF/Et_2O (1:1), affording a crystalline solid showing an 85:15 *RS,SR*:*RR,SS* ratio. By further recrystallization from a CH_2Cl_2/*n*-hexane mixture, this ratio was improved to over 95:5. At this stage, crystals were used for X-ray analysis. Anal. Calcd for $C_{76}H_{62}Fe_2NiO_4P_4\cdot 2CH_2Cl_2$: C, 62.31; H, 4.42. Found: C, 61.78; H, 4.23. ^{1}H NMR (200 MHz, CD_2Cl_2): δ 7.56–6.97 (m, 50 H, Ph), 4.51 (d, 10 H, Cp, ^3J(P–H) = 1.2 Hz), [4.51 (d, 10 H, Cp, ^3J(P–H) = 1.2 Hz)], 3.48 (filled-in d, 2 H, PCH, ^2J(P–H) = 3.2 Hz), [3.40 (filled-in d, 2 H, PCH, ^2J(P–H) = 3.1 Hz)]. The values in square brackets are for the *RR,SS* diastereoisomer. $^{31}P\{^1H\}$ NMR (CD_2Cl_2): δ 78.7 (s, P1), 36.8 (s, P2). IR (Nujol): ν(CO) 1916 (vs) cm^{-1}.

X-ray Data Collection, Structure Solution, and Refinement. A Philips PW 1100 diffractometer was used for the measurements of the data for **3**. The 1810 unique data observed [$I > 2\sigma(I)$] were collected with the use of the $\omega/2\theta$ scanning technique and graphite-monochromated Mo Kα radiation. The pertinent data are summarized in Table I. The structure was solved by the heavy-atom method (Patterson and Fourier synthesis) and anisotropically refined by full-matrix least squares. All the hydrogen atoms were located in a difference Fourier map and introduced as fixed contributors in the final stage of the refinement. During the refinement, a geometrical constraint was applied to the Cp and Ph rings (absolute configuration unambiguously established). The final positional parameters are given in Table II.

A Siemens AED diffractometer was used for the measurements of the data for **5**. The 5320 unique data observed [$I > 2\sigma(I)$] were collected with the use of the $\theta/2\theta$ scanning technique and Nb-filtered Mo Kα radiation. The structure was solved by direct methods (MULTAN) and refined by blocked full-matrix least squares, anisotropically for all non-hydrogen atoms excepting those of the methylene chloride molecules which were treated isotropically. All the hydrogen atoms were located in a difference Fourier map and introduced as fixed contributors in the final stage of the refinement. During the refinement, a geometrical constraint was applied to the Cp and Ph rings. The final positional parameters are given in Table III. Tables of bond distances and angles, thermal parameters, hydrogen atomic coordinates, and structure factor amplitudes are available for both compounds (see paragraph at end of paper regarding supplementary material).

Results and Discussion

The reactions are summarized in Scheme I. The structure of the phosphine ligand $(\eta\text{-}C_5H_5)Fe(CO)(PPh_3)C(O)CH_2PPh_2$ (**3**) has been determined by X-ray analysis (Figure 1). The diastereotopic nature of the PCH_2 protons is evidenced by their occurrence as an ABX pattern in the ^{1}H NMR spectrum, with a very small coupling to the vicinal P atom, as observed in other β-carbonyl phosphines.[6] The geometry about the iron center is pseudooctahedral, similar to that reported for the related compounds [Fe]–COCH(Me)Et,[7a] [Fe]–$COCH_2CH(OH)Et$,[7b] and [Fe]–$C(CH_2)OZr(Cl)Cp_2$ (Cp = $\eta\text{-}C_5H_5$)[4] [P1–Fe–C6 = 91.7 (2), P1–Fe–C7 = 90.0 (2), and C6–Fe–C7 = 95.1 (3)°].[7c] The acyl chain shows an anti conformation about the C7–C8 bond, the torsion angle O2–C7–C8–P2 of −115.5 (6)° resulting in an O2···P2 distance of 3.711 (5) Å. This conformation could result from intramolecular hydrogen-bonding interactions between the acyl oxygen and the α-hydrogen atoms of two phenyl rings [C12H12···O2 = 3.224 (5) Å, C12–H12···O2 = 154°; C52H52···O2 = 3.315 (7) Å, C52–H52···O2 = 134°]. The distance of C7 to the C31–C36 plane is 2.960 (6) Å, and the dihedral angle between this plane and the C7,C8,O2 plane is 149.0 (4)°.

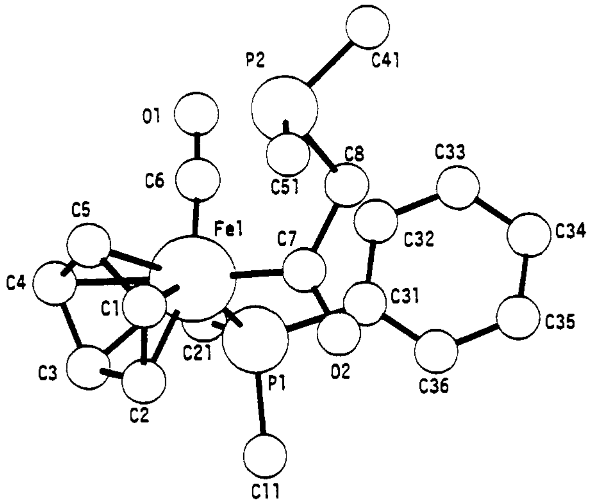

Figure 1. PLUTO drawing of complex **3** showing the atom-labeling scheme (30% probability ellipsoids). Selected bond distances (Å): Fe–P1 = 2.198 (2), Fe–C6 = 1.718 (6), Fe–C7 = 1.964 (6), Fe–Cp1 = 1.748 (6), O2–C7 = 1.225 (7), C7–C8 = 1.514 (9), P2–C8 = 1.852 (6), P2–C41 = 1.852 (5), P2–C51 = 1.839 (5).

The lithium enolate **4** derived from **3** was reacted with nickel chloride. The resulting red-orange crystalline product **5** contained a 70:30 mixture of the two diastereoisomers *RS,SR* and *RR,SS*, as shown by ^{1}H NMR spectroscopy. Purification by successive recrystallizations led to a ratio of 95:5. Each diastereoisomer shows in the ^{1}H NMR a "filled-in" doublet for the PC*H* proton, at δ 3.48 and 3.40 ppm, respectively, characteristic of a cis P–Ni–P arrangement. A cis structure was also found for the related complexes $M[Ph_2PCH{=}C(O)Ph]_2$ (M = Ni, Pd, Pt),[8,9] but the PC*H* resonance was observed between 4.55 and 4.82 ppm. The IR absorption assigned to ν(C$\overset{\dots}{-}$O) + ν(C$\overset{\dots}{-}$C) is observed at 1435 cm^{-1}, against 1515 cm^{-1} in *cis*-$\{Ni[Ph_2PCH{=}C(O)Ph]_2\}$.[8] These data would be consistent with a stronger donor effect of the $CpFe(CO)(PPh_3)$ moiety, compared to Ph. The $^{31}P\{^1H\}$ NMR chemical shift of P2 in **5** (*RS,SR*) is 36.8 ppm, to be compared with the value of 28.2 ppm for *cis*-$\{Ni[Ph_2PCH{=}C(O)Ph]_2\}$. The spectroscopic data in solution are consistent with the results of the crystal structure determination of **5** (*RS,SR*) (Figure 2). The nickel atom has a distorted square-planar coordination, with the metal being out of the mean plane passing through the atoms O2, C7, C8, and P2 by 0.371 (1) and 0.255 (1) Å for the atoms labeled A and B, respectively. The cis arrangement of the ligands allows intramolecular interactions between the acyl oxygen and the α-hydrogen atoms of adjacent phenyl rings: C16AH16A···O2A = 3.110 (8) Å, C16A–H16A···O2A = 139°; C36BH36B···O2B = 3.062 (8) Å, C36B–H36B···O2B = 157°. As expected in the conversion from the keto to the enolato form, the P2–C8 and C8–C7 distances become shorter, and O2–C7 becomes longer in **5** compared to in **3**. Coordination of the phosphino enolate requires a rotation of ca. 110° about the C7–C8 bond when compared to

---

(6) Braunstein, P.; Gomes Carneiro, T. M.; Matt, D.; Balegroune, F.; Grandjean, D. *J. Organomet. Chem.* **1989**, *367*, 117.

(7) (a) Baird, G. J.; Bandy, J. A.; Davies, S. G.; Prout, K. *J. Chem. Soc., Chem. Commun.* **1983**, 1202. (b) Davies, S. G.; Dorder, I. M.; Warner, P. *Ibid.* **1984**, 956. (c) See also: Malisch, W.; Blau, H.; Blank, K.; Krüger, C.; Liu, L. K. *J. Organomet. Chem.* **1985**, *296*, C32.

(8) Braunstein, P.; Matt, D.; Nobel, D.; Balegroune, F.; Bouaoud, S.-E.; Grandjean, D.; Fischer, J. *J. Chem. Soc., Dalton Trans.* **1988**, 353.

(9) Qichen, H.; Minzhi, X.; Yanlong, Q.; Weihua, X.; Meicheng, S.; Youqi, T. *J. Organomet. Chem.* **1985**, *287*, 419.

Table II. Fractional Atomic Coordinates ($\times 10^4$) for Complex **3**

atom	*x/a*	*y/b*	*z/c*	atom	*x/a*	*y/b*	*z/c*
Fe	-1177 (1)	675 (1)	-5101 (0)	C24	-6205 (3)	-329 (3)	-3943 (2)
P1	-1790 (2)	-167 (1)	-4312 (1)	C25	-5394 (3)	-1051 (3)	-3746 (2)
P2	562 (2)	-194 (2)	-6486 (1)	C26	-4067 (3)	-1018 (3)	-3872 (2)
O1	-2790 (5)	-385 (4)	-5924 (2)	C31	-1288 (4)	-1402 (2)	-4355 (2)
O2	1288 (4)	-36 (4)	-4831 (2)	C32	-1938 (4)	-1977 (2)	-4769 (2)
C1	71 (6)	1787 (4)	-5345 (3)	C33	-1517 (4)	-2895 (2)	-4864 (2)
C2	-245 (6)	1855 (4)	-4716 (3)	C34	-446 (4)	-3238 (2)	-4545 (2)
C3	-1610 (6)	1973 (4)	-4667 (3)	C35	204 (4)	-2663 (2)	-4131 (2)
C4	-2137 (6)	1979 (4)	-5266 (3)	C36	-217 (4)	-1745 (2)	-4035 (2)
C5	-1099 (6)	1864 (4)	-5685 (3)	C41	1032 (5)	-1226 (3)	-6948 (2)
C6	-2115 (7)	19 (5)	-5589 (3)	C42	176 (5)	-1509 (3)	-7406 (2)
C7	380 (6)	-108 (4)	-5189 (3)	C43	461 (5)	-2293 (3)	-7761 (2)
C8	566 (6)	-761 (5)	-5726 (3)	C44	1604 (5)	-2795 (3)	-7660 (2)
C11	-1207 (4)	217 (3)	-3565 (2)	C45	2460 (5)	-2512 (3)	-7202 (2)
C12	107 (4)	437 (3)	-3504 (2)	C46	2174 (5)	-1728 (3)	-6846 (2)
C13	602 (4)	694 (3)	-2936 (2)	C51	2100 (5)	460 (4)	-6504 (3)
C14	-215 (4)	732 (3)	-2428 (2)	C52	3062 (5)	425 (4)	-6057 (3)
C15	-1528 (4)	512 (3)	-2490 (2)	C53	4196 (5)	949 (4)	-6126 (3)
C16	-2024 (4)	254 (3)	-3058 (2)	C54	4368 (5)	1508 (4)	-6642 (3)
C21	-3552 (3)	-263 (3)	-4197 (2)	C55	3406 (5)	1542 (4)	-7090 (3)
C22	-4363 (3)	459 (3)	-4394 (2)	C56	2272 (5)	1018 (4)	-7021 (3)
C23	-5690 (3)	426 (3)	-4268 (2)				

Table III. Fractional Atomic Coordinates ($\times 10^4$) for Complex **5**

atom	*x/a*	*y/b*	*z/c*	atom	*x/a*	*y/b*	*z/c*
Ni	2207 (1)	2541 (1)	1888 (1)	O1B	-965 (5)	929 (5)	1350 (7)
Fe1	4494 (1)	2768 (1)	4576 (1)	O2B	1590 (4)	2096 (4)	2630 (5)
Fe2	480 (1)	1159 (1)	3013 (1)	C1B	831 (5)	741 (5)	4454 (5)
P1A	4992 (1)	1707 (2)	3544 (2)	C2B	383 (5)	161 (5)	3557 (5)
P2A	3082 (1)	3075 (1)	1298 (2)	C3B	783 (5)	-29 (5)	2618 (5)
O1A	3377 (4)	1914 (5)	5238 (6)	C4B	1478 (5)	434 (5)	2935 (5)
O2A	2961 (4)	2740 (4)	3264 (5)	C5B	1508 (5)	909 (5)	4069 (5)
C1A	5643 (4)	3154 (5)	5486 (8)	C6B	-384 (7)	1033 (6)	2035 (9)
C2A	5104 (4)	3289 (5)	6254 (8)	C7B	971 (6)	1654 (5)	2077 (8)
C3A	4506 (4)	3803 (5)	5942 (8)	C8B	755 (6)	1524 (6)	933 (8)
C4A	4675 (4)	3985 (5)	4982 (8)	C11B	-271 (4)	3047 (4)	3372 (6)
C5A	5378 (4)	3584 (5)	4700 (8)	C12B	-858 (4)	2861 (4)	2400 (6)
C6A	3818 (6)	2254 (6)	4950 (8)	C13B	-1214 (4)	3448 (4)	1953 (6)
C7A	3706 (5)	2887 (5)	3262 (8)	C14B	-984 (4)	4220 (4)	2479 (6)
C8A	3892 (5)	3107 (6)	2403 (8)	C15B	-397 (4)	4406 (4)	3451 (6)
C11A	4346 (3)	989 (3)	2416 (4)	C16B	-41 (4)	3819 (4)	3898 (6)
C12A	4693 (3)	396 (3)	1655 (4)	C21B	-796 (3)	2218 (4)	4675 (5)
C13A	4218 (3)	-143 (3)	775 (4)	C22B	-979 (3)	1513 (4)	4822 (5)
C14A	3394 (3)	-91 (3)	655 (4)	C23B	-1612 (3)	1469 (4)	5352 (5)
C15A	3046 (3)	501 (3)	1416 (4)	C24B	-2063 (3)	2131 (4)	5735 (5)
C16A	3522 (3)	1041 (3)	2296 (4)	C25B	-1880 (3)	2836 (4)	5588 (5)
C21A	5715 (3)	1874 (4)	2750 (5)	C26B	-1246 (3)	2879 (4)	5058 (5)
C22A	6517 (3)	1963 (4)	3241 (5)	C31B	795 (3)	2806 (4)	5292 (4)
C23A	7057 (3)	2150 (4)	2657 (5)	C32B	589 (3)	3109 (4)	6362 (4)
C24A	6796 (3)	2247 (4)	1583 (5)	C33B	1143 (3)	3532 (4)	7272 (4)
C25A	5994 (3)	2158 (4)	1092 (5)	C34B	1902 (3)	3653 (4)	7112 (4)
C26A	5454 (3)	1971 (4)	1675 (5)	C35B	2108 (3)	3351 (4)	6043 (4)
C31A	5536 (4)	1087 (4)	4391 (5)	C36B	1554 (3)	2928 (4)	5133 (4)
C32A	6055 (4)	506 (4)	3938 (5)	C41B	1577 (4)	1516 (3)	-892 (4)
C33A	6415 (4)	15 (4)	4568 (5)	C42B	1647 (4)	711 (3)	-1104 (4)
C34A	6256 (4)	107 (4)	5651 (5)	C43B	1865 (4)	257 (3)	-2114 (4)
C35A	5737 (4)	688 (4)	6103 (5)	C44B	2012 (4)	607 (3)	-2912 (4)
C36A	5377 (4)	1178 (4)	5473 (5)	C45B	1942 (4)	1411 (3)	-2701 (4)
C41A	3430 (4)	2567 (3)	-7 (4)	C46B	1725 (4)	1866 (3)	-1690 (4)
C42A	3537 (4)	1766 (3)	-219 (4)	C51B	597 (4)	2778 (4)	-84 (6)
C43A	3850 (4)	1339 (3)	-1167 (4)	C52B	576 (4)	3547 (4)	589 (6)
C44A	4054 (4)	1714 (3)	-1904 (4)	C53B	23 (4)	4065 (4)	237 (6)
C45A	3947 (4)	2515 (3)	-1692 (4)	C54B	-509 (4)	3814 (4)	-786 (6)
C46A	3635 (4)	2942 (3)	-744 (4)	C55B	-488 (4)	3045 (4)	-1458 (6)
C51A	2880 (4)	4051 (3)	1161 (5)	C56B	65 (4)	2527 (4)	-1107 (6)
C52A	2291 (4)	4167 (3)	293 (5)	C1S	7436 (14)	1576 (14)	8254 (20)
C53A	2128 (4)	4916 (3)	197 (5)	Cl1S	6776 (4)	2359 (4)	8384 (5)
C54A	2554 (4)	5548 (3)	970 (5)	Cl2S	8169 (4)	1602 (4)	9328 (6)
C55A	3143 (4)	5432 (3)	1838 (5)	C2S	7926 (13)	5419 (13)	5913 (18)
C56A	3306 (4)	4683 (3)	1934 (5)	Cl3S	8477 (4)	4975 (4)	6710 (5)
P1B	80 (2)	2282 (2)	4039 (2)	Cl4S	7257 (5)	4782 (5)	4795 (7)
P2B	1290 (1)	2102 (2)	415 (2)				

3, as indicated by the values of the torsion angles O2–C7–C8–P2 [−5.8 (12) and −8.4 (12)° for **5** vs −115.5 (6)° for **3**], resulting in P2⋯O2 bite distances of 2.749 (7) and 2.728 (7) Å.

We are currently investigating the reactivity of these heterotrinuclear phosphino enolate complexes, which carry a chiral auxiliary, toward electrophilic reagents (e.g., Michael acceptors)

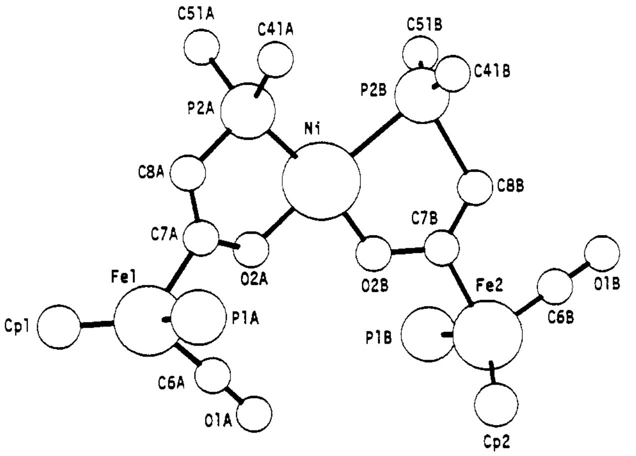

Figure 2. PLUTO drawing of complex **5** showing the atom-labeling scheme (30% probability ellipsoids). Selected bond distances (Å) and angles (deg): Ni–P2A = 2.175 (3), Ni–O2A = 1.903 (5), Ni–P2B = 2.167 (2), Ni–O2B = 1.881 (7), Fe1–P1A = 2.198 (2), Fe1–C6A = 1.734 (12), Fe1–C7A = 1.979 (9), Fe1–Cp1A = 1.748 (10), O2A–C7A = 1.324 (11), C7A–C8A = 1.346 (11), P2A–C8A = 1.758 (8), P2A–C41A = 1.816 (6), P2A–C51A = 1.821 (6), Fe2–P1B = 2.204 (2), Fe2–C6B = 1.716 (10), Fe2–C7B = 1.989 (12), Fe2–Cp1B = 1.732 (10), O2B–C7B = 1.318 (11), C7B–C8B = 1.363 (13), P2B–C8B = 1.754 (12), P2B–C41B = 1.808 (5), P2B–C51B = 1.814 (7), P2B–Ni–O2B = 84.4 (2), O2A–Ni–O2B = 85.3 (3), P2B–Ni–O2A = 167.9 (2), P2A–Ni–O2B = 169.8 (2), P2A–Ni–P2B = 105.6 (1), P2A–Ni–O2A = 84.5 (2).

in order to generate C–C or C–element bonds with high stereoselectivity.

Acknowledgment. We thank the Fonds National Suisse de la Recherche Scientifique (Grant No. 20-26245.89) and the CNRS for financial support and the Université Louis Pasteur for a Visiting Professorship to C.F.

Supplementary Material Available: For compounds **3** and **5**, tables of crystal data, data collection, and solution and refinement parameters, bond distances and angles, thermal parameters, and hydrogen atomic coordinates and Figure S1, showing the structure of **3** with the complete numbering scheme and Newman projection looking from the α-carbon C(7) to the metal, and Figure S2, giving the structure of **5** showing the environment of the metals and the arrangement of the phenyl rings (14 pages); tables of observed and calculated structure factors (22 pages). Ordering information is given on any current masthead page.

Contribution from the Institute for Inorganic Chemistry,
University of Munich, Meiserstrasse 1, 8000 Munich 2, FRG

Influence of Hydrogen Bonding on the Molecular Geometry and Solution-State NMR Properties of $[\mathrm{tmpH_2}][\mathrm{Me_3SnCl_2}]$[1]

Stephen E. Johnson,*[2] Kurt Polborn, and Heinrich Nöth*

Received July 17, 1990

Recently, we have observed some interesting structural distortions from the idealized trigonal-bipyramidal geometry for a pentacoordinate triorganotin(IV) anion possessing a cation capable of extensive hydrogen-bonding interactions, a type of complex not observed for tin until now. Studies of pentacoordinated tin compounds are of special significance in structural tin chemistry[3] in view of the implication that five-coordinate tin(IV) intermediates are formed during substitution reactions of organotin compounds. An intimate knowledge of the structural details, therefore, is quite significant in order to understand the nature of the bonding in these compounds and to observe the manner in which the molecular geometry of the pentacoordinated state is influenced by effects such as hydrogen bonding through direct anion–cation interactions.

Experimental Section

Physical Measurements. NMR spectra were obtained by using Bruker AC 200-MHz, JEOL FX 90-MHz, and JEOL 270-MHz spectrometers. ^{1}H and ^{13}C chemical shifts were referenced to internal $\mathrm{CDCl_3}$. ^{119}Sn chemical shifts were referenced to external $\mathrm{Me_4Sn}$. FT-IR spectra were obtained on a Nicolet spectrometer using Nujol and Hostaflon matrices. Elemental analyses were performed at the University of Munich microanalysis laboratory.

Preparation of $[\mathrm{tmpH_2}][\mathrm{Me_3SnCl_2}]$ (1). A mixture of $\mathrm{Me_3SnCl}$ (2.51 g, 12.6 mmol) in 20 mL of $\mathrm{CH_3CN}$ and an equivalent amount of $[\mathrm{tmpH_2}][\mathrm{Cl}]$ (2.24 g, 12.6 mmol) in 30 mL of $\mathrm{CH_3CN}$ were stirred at ambient temperature for 24 h. Concentration of solvent from the reaction mixture in vacuo results in the desired product **1**. A total of 4.72 g (92% yield) of product is obtained, having mp 244–248 °C. The compound is hygroscopic but can be handled indefinitely in the absence of moisture. $^1\mathrm{H}(\mathrm{CDCl_3})$: 0.681 (s, $\mathrm{Me_3Sn}$–, $^2J(^1\mathrm{H}-^{119}\mathrm{Sn}) = 60.0$ Hz, $^2J(^1\mathrm{H}-^{117}\mathrm{Sn}) = 56.9$ Hz, 9 H); 1.58 (s, $\mathrm{CH_3}$/tmp, 12 H); 1.72 (s, $-\mathrm{CH_2}-$/tmp, 6 H); 8.42 (br s, NH proton/tmp, 2 H). $^{13}\mathrm{C}(\mathrm{CDCl_3})$: 0.049 (s, $^1J(^{13}\mathrm{C}-^{119}\mathrm{Sn}) = 400$ Hz, $^1J(^{13}\mathrm{C}-^{117}\mathrm{Sn}) = 380$ Hz). $^{119}\mathrm{Sn}(\mathrm{CDCl_3}$, 303 K): 153.7 (s). $^{119}\mathrm{Sn}(\mathrm{CDCl_3}$, 213 K): 101.3 (br s). Anal. Calcd for $\mathrm{C_{12}H_{27}Cl_2SnN}$: C, 38.23; H, 7.77; N, 3.71. Found: C, 38.89; H, 8.20; N, 4.05.

X-ray Structural Data for 1. The compound $[\mathrm{tmpH_2}][\mathrm{Me_3SnCl_2}]$ crystallizes in the monoclinic space group $P2_{1/n}$[4a] with $a = 13.884$ (2) Å, $b = 7.694$ (2) Å, $c = 17.109$ (2) Å, $\beta = 90.448$ (2)°, $Z = 4$, and $\mu_{\mathrm{Mo\,K\alpha}} = 16.807\ \mathrm{cm^{-1}}$. The crystal used in the X-ray study had maximum dimensions of approximately 0.20 mm × 0.27 mm × 0.20 mm. A total of 2240 independent reflections ($\pm h,+k,+l$) were measured at 23 ± 1 °C, by using the $\theta-2\theta$ scan mode and graphite-monochromated Mo Kα radiation ($\lambda = 0.71073$ Å), for $4° \le 2\theta \le 46°$, on an Enraf-Nonius CAD-4 diffractometer. No corrections were made for absorption. The structure was solved by using heavy-atom methods and difference Fourier techniques. Full-matrix least-squares refinement (non-hydrogen atoms anisotropic, methyl and tmp ring hydrogens riding isotropic, function minimized $\sum w(|F_\mathrm{o}| - |F_\mathrm{c}|)^2$, $w^{1/2} = 2F_\mathrm{o}L_\mathrm{p}/\sigma_I$) led to a conventional unweighted residual $R = \sum ||F_\mathrm{o}| - |F_\mathrm{c}||/\sum |F_\mathrm{o}|$ of 0.0470 and $R_\mathrm{w} = 0.0384$ for the 1800 reflections having $I \ge 2\sigma_I$. Mean atomic scattering factors were taken from ref 4b. Real and imaginary dispersion corrections for Sn, N, and Cl were taken from the same source (pp 149–150). Calculations were performed on a Microvax II computer using the Enraf-Nonius CAD-4 SDP system of programs package.

Results and Discussion

The reaction of equivalent amounts of trimethyltin chloride with 2,2,6,6-tetramethylpiperidinium chloride, $[\mathrm{tmpH_2}][\mathrm{Cl}]$, in acetonitrile solution proceeds according to eq 1 to result in formation

$$\mathrm{Me_3SnCl + C_9H_{18}NH_2Cl \rightarrow [C_9H_{18}NH_2][Me_3SnCl_2]} \tag{1}$$

of the pentacoordinated tin complex, $[\mathrm{Me_3SnCl_2}][\mathrm{tmpH_2}]$, in high yield. The anionic tin(IV) complex was first isolated, in good yield, from the novel reaction of a stannyl-functionalized diazadiboretidine, $[\mathrm{Me_3SnN{=}B{-}Ntmp}]_2$, with methylene chloride or chloroform solvent over time.[5] Colorless, parallelepipeds of $[\mathrm{tmpH_2}][\mathrm{Me_3SnCl_2}]$ suitable for an X-ray experiment were grown from $\mathrm{CH_2Cl_2}$ solution.

As shown in Figure 1, the anion can be considered as an axially distorted trigonal-bipyramidal structure of C_{3v}–$3m$ symmetry with three methyl groups located at equatorial sites and two chlorine atoms axially oriented. The three Sn–C bond lengths are all within 0.01 Å of the value of 2.121 (8) Å. The three C–Sn–C bond angles are all within 0.9° of the average value of 118.5 (3)°. The Cl(1)–Sn–Cl(2) fragment is essentially linear at tin, whereas the

---

* To whom correspondence should be addressed.

[1] Presented in part at the 200th National Meeting of the American Chemical Society, Washington DC, Aug 1990; paper INOR 31.

[2] National Science Foundation Post-Doctoral Fellow. Current address: Department of Chemistry and Biochemistry, University of California at Los Angeles, 405 Hilgard Ave., Los Angeles, CA 90024.

[3] (a) Zubieta, J. A.; Zuckerman, J. J. *Prog. Inorg. Chem.* **1978**, *24*, 251. (b) Holmes, R. R. *Prog. Inorg. Chem.* **1984**, *32*, 119. (c) Harrison, P. G. In *The Chemistry of Tin*; Harrison, P. G., Ed.; Blackie: London, 1989.

[4] (a) *International Tables for X-ray Crystallography*; Kynoch: Birmingham, England, 1974; Vol. I, p 99. (b) *Ibid.*; Kynoch: Birmingham, England, 1974; Vol. IV, pp 72–98.

[5] Johnson, S. E.; Noeth, H. Unpublished results. Details of this work will be published elsewhere.